IX CONGRESSO BRASILEIRO DE
ENGENHARIA E CIÊNCIAS TÉRMICAS

9th BRAZILIAN CONGRESS OF THERMAL
ENGINEERING AND SCIENCES

Paper CIT02-0304

NUMERICAL STUDY OF TURBULENT BOUNDARY LAYER FLOWS OVER ROUGH SURFACES – PART I: VELOCITY PROFILES

Mila R. Avelino[1]
Department of Mechanical Engineering
University of Miami, Coral Gables, FL, USA
mila@uerj.br

Atila P. Silva Freire
Mechanical Engineering Program
Federal University of Rio de Janeiro – COPPE/UFRJ
Rio de Janeiro, RJ, Brazil
atila@serv.com.ufrj.br

Marcelo J.S. de Lemos
Departamento de Energia - IEME
Instituto Tecnológico de Aeronáutica - ITA
12228-900, São José dos Campos, SP, Brazil
delemos@mec.ita.br

Abstract. The effects of sudden changes are predicted in the cases of turbulent flow around surface-mounted two-dimensional ribs when subjected to a sudden change in surface roughness. A particular interest of this study is to investigate the sudden changes in the surface roughness for developing boundary layer flow. A two-equation k-ε turbulence model is employed to simulate the turbulent transport. Equations of boundary-layer type were used and a forward marching method was employed for sweeping the computational domain. Wall functions that take into account surface roughness are used to specify the boundary conditions at the surface. The effects of the sudden changes of roughness accounted for the wall functions in the k-ε turbulence model are compared with available experimental data. Four configurations are simulated here, namely one extensive uniformly smooth surface, and three cases where the surface roughness varies suddenly from a smooth to rough, each one being with a different roughness geometry. For the vicinities of the surface change algebraic expressions are empirically obtained to predict the growth of the displacement in origin. Those heuristic expressions are incorporated into the numerical code to predict the velocity profiles more accurately. Results are presented for velocity and skin friction coefficient, in addition to comparisons with experimental data. The use of the algebraic expressions in a parabolic solver showed good agreement with experimental values for the mean and local quantities.

Keywords: *Turbulent Flow, Numerical Study, Surface Roughness.*

1. Introduction

The present work is concerned with flows that develop over flat surface with changing surface conditions. In particular, we will be looking at flows that present abrupt changes in wall roughness. The theory to be used here is, therefore, expected to account for these effects. Here, we will use the k-ε model to describe the properties of the boundary layer in the surface layer, and validated the results against the experimental data of Avelino (2000).

The k-ε model will use a wall function to represent the velocity profile near the wall so that a local analytical solution for the inner region will be used as a boundary condition for the outer solution. This inner solution must take into account the local changes in the flow such as those caused by the changes on the surface roughness (Avelino et al, 2001). The local changes are then accounted for by logarithmic profiles that take as a characteristic length the displacement in origin, which has been experimentally studied by Avelino et al. (1998).

In the present work algebraic expressions that predict the behaviour of the displacement in origin when the flow is subject to sudden changes of surface roughness are incorporated into the numerical code. In previous works, Avelino et al. (2001a, 2001b) a numerical study of the k-ε model for flows with step changes in surface roughness were carried out. Appropriate boundary conditions with dependence on the displacement in origin were made use of, and numerical simulation showed reasonable agreement with the experimental data.

[1]Visiting Scholar from: Departamento de Engenharia Mecânica, Unversidade do Estado do Rio de Janeiro – UERJ, 20550-013 - Rio de Janeiro, RJ, Brazil

The use of simple numerical tools for preliminary engineering design, instead of using memory-demanding, large Computational Fluid Dynamics (CFD) codes, can benefit the overall design process if repetitive calculations are mandatory. If no back flow is in order, marching-forward techniques, implemented along with isotropic turbulence models, provide an economical means for conceptual design using cheaper PC-based workstations.

Acknowledging the advantages of "fast" parabolic solvers, the work of Matsumoto & de Lemos (1990), presented results for the developing time-averaged and turbulent fields in a coaxial jet along a circular duct of constant area. Later, de Lemos & Milan (1997), extended their calculations to flow in long ducts through varying cross sections. Similar results for ducts with plane walls have also been documented in Braga & de Lemos (1999). The numerical methodology developed in all of that work is here employed. There, use was made of the isotropic k-ε model and the wall log-law for velocity over smooth surfaces. Therefore, the present calculations used additional wall laws in order to account for rough walls.

For flows over rough surfaces, the number of studies is limited. Studies on flows over rough surfaces with changes in the thermal boundary conditions were made by Coleman et al.(1976) and by Ligrani et al.(1979, 1983,1985).

2. Mean Flow and Turbulence

The geometry investigated is next detailed, followed by the governing equations, the numerical method used and the results obtained. Four geometrical configurations will be considered and analysed using boundary layer equations, one reference case, in which the surface is smooth, and three geometry configurations where abrupt change of surface roughness is imposed to the flow are presented.

2.1. Geometry

The flow here analyzed consists of a confined stream inside a rectangular channel of constant cross section. Situations concerning surface roughness variation along the longitudinal coordinate are also considered. A schematic of the configuration under study is shown in Fig. 1. A wind tunnel of 30x30 cm of cross section and 2 m long has the bottom surface made rough with the help of transverse aluminum ribs. Four configurations were placed in the wind tunnel by alternating the position of the rough elements in the test section. The smooth surface was simulated as a

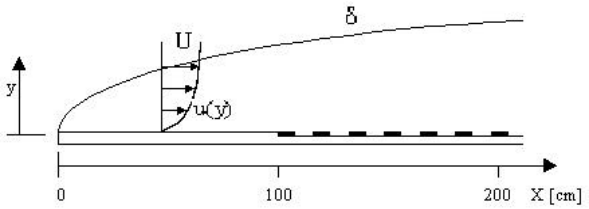

Fig. 1 – Coordinate system for the smooth to rough surface.

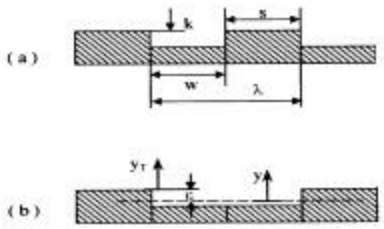

Fig. 2-Rough surface geometry and coordinate system displacement of origin.

reference case over a glass surface. In the other three configurations, the rough surfaces adopted were composed of transversally grooved surfaces with rectangular slats in different geometries. For more details about the experimental work see Avelino(2000) and Guimaraes et al.(1999).

. The rough surface is schematically shown in Fig. 2 together with the diagrammatic definition of the displacement in origin, $\hat{I}$. The parameters in Fig. 2 are specified in Table 1 for the three rough surfaces studied here.

In the vicinities of the abrupt change, the flow experiences a transition from one extensive region to another, being affected by the new geometry, until it reaches the fully rough regime. In previous works, Avelino et al.(2001a, 2001b) the theory used did not represent the transition region from one extensive surface condition to another. In the region where the flow had already reached the fully rough regime, the numerical prediction showed good agreement with the experimental results. Here, intending to improve the accuracy of the simulations on the vicinities of the sudden change in the wall roughness, algebraic expressions derived from experimental data are incorporated into the code. By using the expressions heuristically derived in the numerical simulation, the growth of $\in$ is taken into account.

Table 1 – Geometry of the roughness elements.

	Rough Surface Type I	Rough Surface Type II	Rough Surface Type III
K [mm]	**4.77**	**4.77**	**6.35**
W [mm]	**15.88**	**31.76**	**15.88**
S [mm]	**15.88**	**15.88**	**4.76**
l [mm]	**31.76**	**47.64**	**20.64**
W/K	**3.33**	**6.66**	**2.5**

Three different roughness configurations are simulated. The dimensions of the three geometry configurations are presented in Table 1. For the roughness elements, K denotes the height, S the length, W the gap, and λ the pitch. Authors (see, e.g., Perry and Joubert(1963), Antonia and Luxton(1971, 1972), Wood and Antonia(1975)) have classified the rough surfaces into two distinct types of surfaces: 1) 'K' type rough surfaces and 2) 'D' type rough surfaces. In the cases where the nature of the roughness can be expressed with the help of a single length scale, the height of the protrusions, 'K', the surface is termed of 'K' type. Flows, on the other hand, which are apparently insensitive to the characteristic scale 'K', but dependent on global parameters of the flow are termed 'D' type flows.

2.2. Boundary Layer Equations

For generality, the equations below are written embracing planar and axis-symmetric cases. The equations are also presented in a simplified form, already making use of the concept of isotropic turbulent viscosity, μ_t.

$$\frac{\partial(r^h\, r\, u)}{\partial x} + \frac{\partial(r^h\, r\, v)}{\partial y} = 0 \quad , \tag{1}$$

$$\rho u\frac{\partial u}{\partial x} + \rho v\frac{\partial u}{\partial y} = -\frac{\partial p}{\partial x} + \frac{1}{r^h}\frac{\partial}{\partial y}\left[r^h\, \mu_{eff}\frac{\partial u}{\partial y}\right]. \tag{2}$$

In Equations (1) and (2) u, v are the velocity components in the axial and transverse direction, respectively, ρ the fluid density, p the static pressure, and μ_{eff} is the effective (turbulent+laminar) coefficient of exchange given as,

$$\mu_{eff} = \mu + \mu_t \,, \tag{3}$$

where μ is the molecular viscosity. As mentioned before, Eqs.(1) and (2) are written in a compact notation embracing planar (η=0) and axi-symmetric (η=1, r=y') cases. Further, in the k-ε model one has (Jones & Launder, 1972),

$$\mu_t = \rho\, c_\mu\, k^2 / \varepsilon \,, \tag{4}$$

where c_μ is a constant. Transport equations for k and ε are written as (Launder & Spalding, 1974),

$$\begin{aligned} \rho u\frac{\partial k}{\partial x} + \rho v\frac{\partial k}{\partial y} &= \frac{1}{r^h}\frac{\partial}{\partial y'}\left[r^h\, G^k_{eff}\frac{\partial k}{\partial y}\right] + S_k \,, \\ \rho u\frac{\partial \varepsilon}{\partial x} + \rho v\frac{\partial \varepsilon}{\partial y} &= \frac{1}{r^h}\frac{\partial}{\partial y}\left[r^h\, G^\varepsilon_{eff}\frac{\partial \varepsilon}{\partial y}\right] + S_\varepsilon \,. \end{aligned} \tag{5}$$

In Equation (5), $G^k_{eff} = \mu + \mu_t/\sigma_k$ and $G^\varepsilon_{eff} = \mu + \mu_t/\sigma_\varepsilon$ where the G's are the effective coefficient of exchange and the σ's are the turbulent Prandtl/Schmidt numbers for k and ε. The last terms in Eq.(5) are known as "source" terms and are given by $S_k = \rho\,(P - \varepsilon)$ and $S_\varepsilon = \rho\, \varepsilon/k\,(c_1 P - c_2 \varepsilon)$ where c_1=1.47, c_2=1.92 and c_μ = 0.09. The production term reads

$$P = \frac{\mu_t}{\rho}\left(\frac{\partial u}{\partial y}\right)^2 . \tag{6}$$

2.3. Coordinate System

The numerical solution of Eqs.(1), (2) and (5) in the coordinate system x-y presents some difficulties in regard to numerical precision. In this system, there is the disadvantage of having only a few nodal points where the boundary layer is "*thin*" and too many points where the thickness of the boundary layer has attained substantial growth. This work uses the coordinate system x-w, proposed in Patankar (1988), by doing;

$$w = \frac{Y - Y_I}{Y_E - Y_I} \,, \tag{7}$$

where Y is the stream function and the subscripts I and E refer to the internal and external boundary layer limiting surfaces, respectively.

The equation set formed by Eqs. (1)-(2)-(5) can be written in the coordinate system *x*-*w* as (Patankar, 1988),

$$\frac{\partial f}{\partial x} + (a + b\,w)\frac{\partial f}{\partial w} = \frac{\partial}{\partial w}\left(c\,\frac{\partial f}{\partial w} \right) + d\,, \tag{8}$$

where,

$$a = -\frac{dY_I}{dx}/Y_{EI}; \quad b = -\frac{dY_{EI}}{dx}/Y_{EI}; \quad c = r^2 r\,u\,G_{eff}^{f}/Y_{EI}^{2}; \quad d = S_f/(r\,u); \quad Y_{EI} = Y_E - Y_I. \tag{9}$$

In Eq. (8), f can represent any of the dependent variables (f =*u*,*k*,*e*), Γ_{eff}^{f} is an effective coefficient of diffusion for f and S_f a source term. The discretization of (8) is obtained through the control volume method (Patankar & Spalding, 1972, Patankar, 1980) implying in (see Fig. 3a for notation),

$$a_P f_P = a_N f_N + a_S f_S + a_{PA} f_{PA} + b_P\,, \tag{10}$$

where the coefficients involve convection, diffusion and source terms. For the solution of system (10) the Three Diagonal Matrix Algorithm is here adopted.

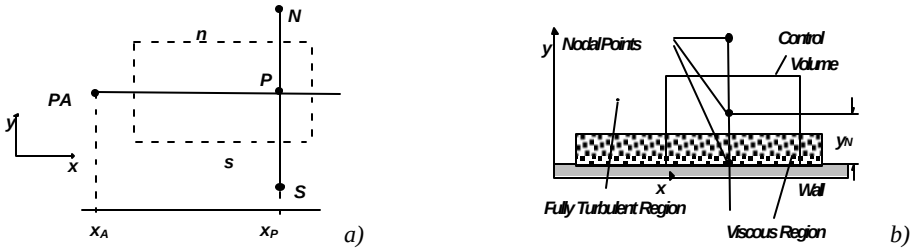

Fig. 3 – General notation for smooth wall model: *a*) Control volume, *b*) wall layer model.

2.4. Inlet Conditions

Inlet flow is given a uniform distribution and the values of k and ε at entrance were assumed as,

$$k_{in} = C\,U_m^2, \quad e_{in} = k_{in}^{3/2}/K\,y\,, \tag{11}$$

where $C = {}^1\!/_2 Tu^{\,2}$, $Tu = \sqrt{3\overline{(u_i')^2}}\Big/U_m$ is the turbulence intensity at inlet, U_m is the overall mean velocity, K is the von Kármán constant (K=0.41) and y the distance to the wall. Halfway to the top surface (*y*=*H*/2) the symmetry condition is implemented for all dependent variables ϕ=u,k,ε, as $\partial f/\partial y\big)_{y=0} = 0$.

2.5. Wall Treatment for Smooth Surfaces

The mathematical model seen above is not valid inside the layers very close to the wall where viscous effects are predominant. Velocity at the grid point closest to the wall is handled by the usual Wall Function approach described in Launder & Spalding (1972). The notation below refers to Fig. 3b where the location of the grid point closest to the wall, *N*, is identified. The wall function gives for the wall shear stress at node *N*,

$$t_w = \left(U_N\, r\, c_m^{1/4} k_N^{1/2}\right) \Big/ \frac{1}{K} \ln\left[E\, y_N \frac{r\,(c_m^{1/2} k_N)^{1/2}}{m} \right], \tag{12}$$

where *E* is a constant. In the wall region, the use of the wall function, characterized by the expressions,

$$U_N^+ = \frac{1}{K}\ln\left(y_N^+ E\right), \tag{13}$$

where

$$U_N^+ = \frac{u_N}{U^*}; \quad y_N^+ = \frac{\rho\, U^* y_N}{\mu}; \quad U^* = \sqrt{\frac{\tau_w}{\rho}}, \tag{14}$$

and the employment of the assumption of "local equilibrium" for turbulence ($P=\varepsilon$), gives for point N,

$$k_N = \tau_w / (\rho c_\mu^{1/2}); \qquad \varepsilon_N = c_\mu^{3/4} k_N^{3/2} \Big/ \kappa y_N \ . \tag{15}$$

2.6. Wall Treatment for Rough Surfaces

The fundamental concepts and ideas on the problem of a fluid flowing over a rough surface were first established by Nikuradse(1933). For rough surfaces Moore(1951) has shown that a universal expression can be written for the wall region by setting the origin for measuring the velocity profile some distance below the crest of the roughness elements. Thus, the equations above for the law of the wall are modified to take into account the effects for roughness. The basic facts about the laws of the wall for the velocity profiles have been discussed elsewhere (see Avelino et al. (1996)). For computing the flow over the rough surface at the bottom of the wind tunnel, Eq. (13) is modified for including the roughness function. Accordingly, an expression for the velocity profile valid for all types of roughness can be written if we make

$$\frac{u}{U^*} = \frac{1}{\kappa}\ln\frac{(y_T + \in)U^* \rho}{\mu} + A - \frac{\Delta u}{U^*}, \tag{16}$$

where,

$$\frac{\Delta u}{U^*} = \frac{1}{\kappa}\ln\frac{\in U^*}{\nu} + C_i \ . \tag{17}$$

In the above equations all symbols have their classical meaning; C_i , i= K, D is a constant characteristic of the type of roughness; the coordinate y_T is the distance measured from the crest of the roughness elements ($y = y_T + \in$); $\in$ is the displacement in origin, referred to in literature as the error in origin as well. Equations (16) and (17) will be used to specify the boundary conditions on a k-ε formulation of the problem. The values for A, C_i and $\in$ used were 5.15, 4.3 and 1.9mm, respectively. Finally, rewriting (12) in the form $\tau_w = l\,\mu(\partial U/\partial y)$ gives further,

$$l = \begin{cases} 1 & \text{for laminar flow} \\ \dfrac{\kappa\, y_N \dfrac{\rho (c_\mu^{1/2} k_N)^{1/2}}{\mu}}{\ln\left[E\, y_N \dfrac{\rho (c_\mu^{1/2} k_N)^{1/2}}{\mu}\right]} & \text{for turbulent flow over smooth surface} \\ \dfrac{\kappa\, y_N \dfrac{\rho (c_\mu^{1/2} k_N)^{1/2}}{\mu}}{\ln\left[E_r \dfrac{y_N}{\in}\right]} & \text{for turbulent flow over rough surface} \end{cases} \tag{18}$$

The domain of validity of (16)-(17) is the fully turbulent region and that can be verified through application of the single limit concept of Kaplun (1967) (see Silva Freire & Hirata, 1990).

2.7. The Displacement in Origin

The determination of the displacement in origin $\in$ is significant for the evaluation of the properties of the flow over a rough surface, including all local and global parameters. All graphical methods for its determination, however, assume the existence of a logarithmic region, which may not occur near to a step change in roughness.

It is known that for turbulent boundary layers developing over rough surfaces, the logarithmic regions of the flow suffer a slight deformation to the left side. In fact, as we shall see, a very popular method to find $\in$ is based on a procedure to restore the lower portion of the velocity profile to a logarithmic profile.

The displacement in origin, $\in$, was estimated by four different procedures. The procedures of Perry and Joubert(1963) and Perry et al.(1987) are the most rigorous that can be found in literature so that the data resulting from them must be seen as reliable. The procedures of Thompson(1978) and Bandyopadhyay(1987) are more simplified so that the values of $\in$ obtained through them must be seen just as a first approximation.

Therefore, to determine the displacement in origin, the velocity profiles were plotted in semi-log form, in dimensional coordinates. Next, the normal distance from the wall was incremented by 0.1mm and a straight line fit was applied to the resulting points. Searching for the maximum coefficient of determination, the best fit was determined. Other statistical parameters were also observed, as the residual sum of squares and the residual mean square.

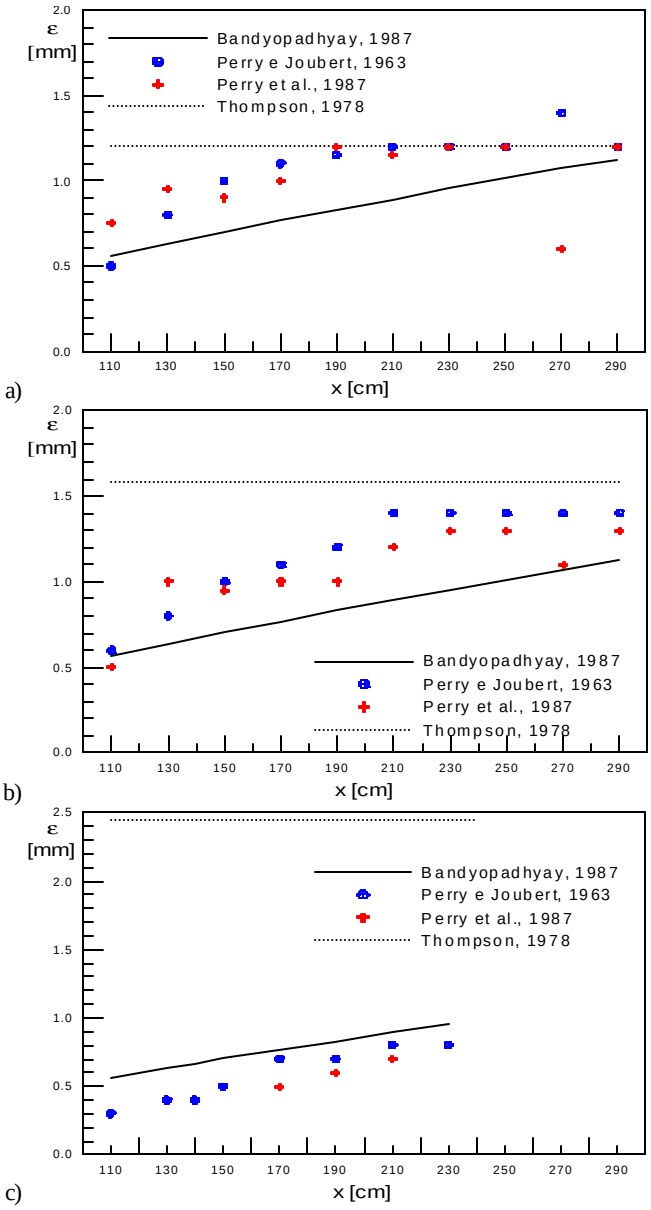

Figure 4 - Displacement in origin for velocity profiles over different rough surfaces of Fig. 2: a) Type I, b) Type II, c) Type III.

Table 2 – Estimated expressions for $\in$ obtained from the experimental data.

	Estimated expressions of $\in$	Estimated values for exponent 'm'
Surface Type I	$\in = 0.0012\ x^m$	m=1.04
Surface Type II	$\in = 0.0118\ x^m$	m=0.81
Surface Type III	$\in = 0.0150\ x^m$	m=0.90

Fig. 4 present the best fits from the experimental displacement in origin data for all the three roughness types summarized in Table 2. The estimated values of $\hat{I}$ were obtained experimentally in Avelino(2000). In the numerical computations the expressions in Table 2 will be used to represent $\hat{I}$. Those expressions are used to predict the abrupt change in the roughness properties in the immediate vicinities of the change in properties at the wall.

Having found $\hat{I}$, the gradient of the log-law is used to determine U^*. Another method to determine U^* is the momentum-integral equation. The results for $\hat{I}$ in the rough surfaces types I, II and III, are presented in Figs. 4 to 6. Considering the high degree of difficulty involved in finding these results, and the reasonable agreement between the predictions based on the two alternative procedures, the results of $\hat{I}$ and consequently for C_f are expected to be representative of the flow.

Figure 4 clearly show that $\in$ represents a relatively quick streamwise evolution for surfaces Types I and II, a fact that has been previously observed in 'K' type rough surfaces. The evolution of $\in$ on surface type III is observed to be rather slower and representative of a 'D' type surface. In Fig. 4c, the value of $\in$ calculated through procedure suggested in Thompson(1978) furnishes $\in$=2.44.

3. Results and Discussion

Numerical results calculated with the model shown above were used to simulate the flow over the flat surface of Figs. 5 to 8. Four cases were investigated and classified according to the rough surface type. Computations used different wall boundary conditions, based on Eq. (18), which were applied over the corresponding surface length detailed in Table 1. Also, for better prediction of the effects provoked by the roughness, algebraic expressions are used according to Fig. 4 and Table 2. The results to follow were compared with measurements of Avelino et al. (1999).

Figures 5 to 8 show comparisons of u/U_m versus y/d, where d is the boundary layer thickness, for the four different cases studied. Profiles at ten longitudinal stations are compared with the numerical prediction showing good agreement. The lines represent the numerical predictions whereas experimental values are plotted with symbols.

Profiles were calculated at stations in the vicinity of the surface conditions variation. In previous work, Avelino et al.(2001a, 2001b), u/Um did not quite match those of the experimental dada, most likely due to the transition region explained earlier, as the value of the displacement in origin was assumed constant. In those works, numerical simulations using the logarithmic expressions were made and it was noticed that although the predictions in the vicinity of the surface change did not match, as the flow approaches an equilibrium condition, the predictions presented reasonable agreement with experimental data. Here, algebraic expressions for prediction of the displacement in origin behavior were incorporated to the numerical code, showing an improve in the prediction of the velocity profiles in the region close to the abrupt change in the surface condition. Even though the fully rough regime had not established.

One interesting feature of Figs. 5 to 8 is that in spite of using a parabolic solver and a linear k-ε model, the present calculation seems to represent quite well the phenomena in the whole extension of the plate.

The discrepancies encountered in previous works, due to the gradual growth of the displacement in origin, until it had reached a constant value, are vanished by the implementation of the expressions for the growth of the displacement in origin in the vicinities of the sudden change in roughness. The velocity profiles are now accurately predicted in the transitional region as well. With the implementation of the expression representing the increase in $\in$, accurate predictions of the development of the boundary layer immediately after the changes in the wall roughness can be observed. In other words, a function of a characteristic length scale of the rough elements can be used for the prediction of the velocity profiles in the transition region of the flow.

Corresponding skin friction coefficient values are shown in Figs. 9a to 9d. In these figures, numerical prediction is compared with those calculated through an integral method and a graphical determination, based on the experimental results. For the case of a uniformly smooth surface, a theoretical correlation is also included.

The values of $\in$ were calculated according to the method of Perry & Joubert (1963). Systematically adding an arbitrary displacement in origin to the original profiles, the least square method could be applied to the near wall points to search for the best straight line fit.

It is clear from Figs. 9a-d that the numerical prediction is in good agreement with the theoretical correlation for turbulent boundary layers over smooth surface, and with the experimental results, either calculated by using the integral balance of the momentum or through the chart method. It can be noticed from Fig. 9, where the step change in roughness is present, that the numerical prediction responds very fast to the new surface condition. Also the momentum balance and the graphical method are in good agreement.

It is known that in the region where the flow leaves a rough surface, to come upon a smooth surface, a departure from experimental values can be observed immediately after the sudden change in the roughness. This fact is due to the transition region that the flow undergoes following the surface step change.

When in contact with a smooth surface, the displacement in origin tends to decrease until it vanishes, and this can be noticed by either the integral method or by the chart method, conversely, in the parabolic solver, this effect cannot be caught. In fact, in the numerical model above, no mechanism that could bring back information from downstream positions is considered. The flow, in this case, can be characterized as of partially parabolic nature requiring an elliptic solver for the pressure field.

For engineering purposes, however, the parabolic treatment has proven to be adequate for reproducing the major features of the flow.

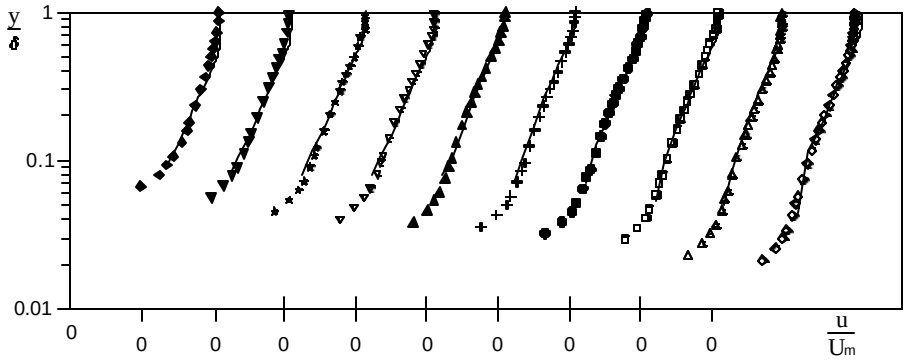

Fig. 5 – Velocity profiles over smooth surface.

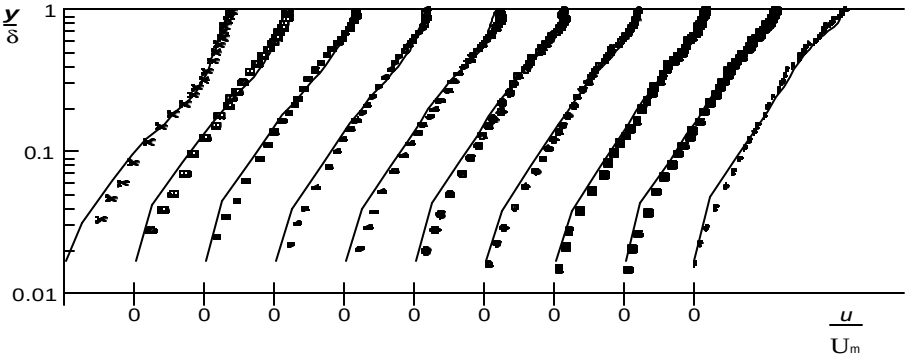

Fig. 6 – Velocity profiles over Type I rough surface.

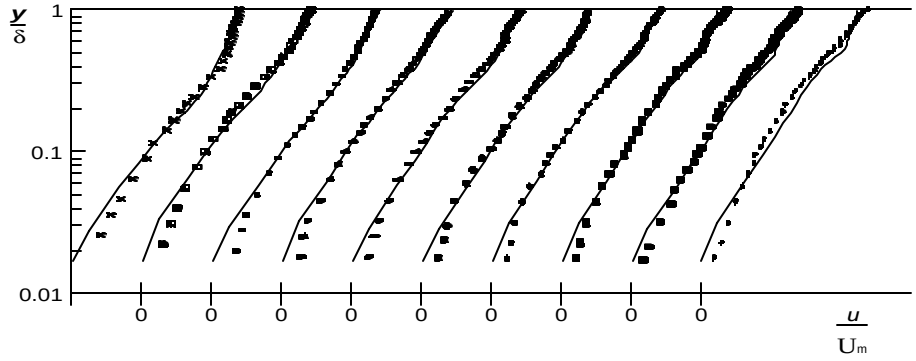

Fig. 7 – Velocity profiles over Type II rough surface.

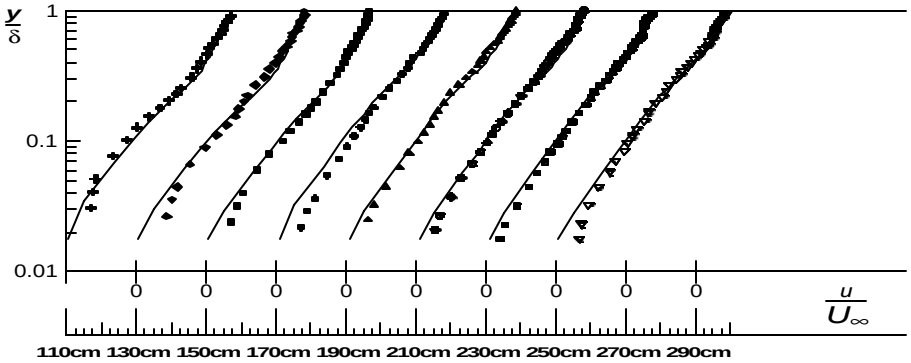

Fig. 8 – Velocity profiles over Type III rough surface.

These results are coherent with the idea of limiting the present model to the regions of the flow where the displacement in origin has already reached a constant value, in the fully rough region of the flow.

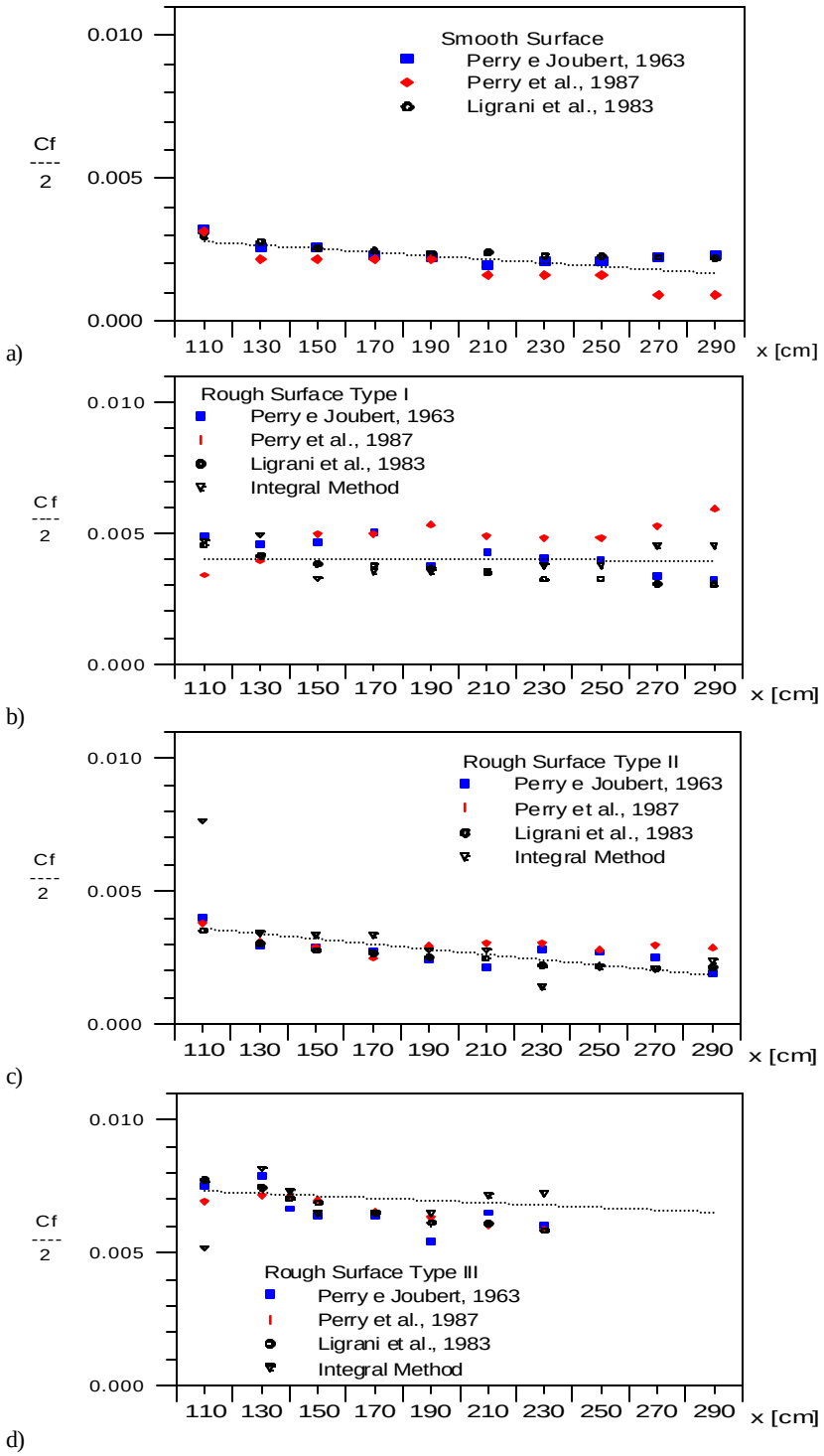

Figure 9 - Skin friction coefficient for flows over surfaces of Fig. 2: a) Smooth, b) Type I, c) Type II, d) Type III.

The determination of the displacement in origin, $\in$, is crucial for the evaluation of the properties of the flow over a rough surface, including all local and global parameters such as, e.g., the skin-friction coefficient and the momentum thickness. All graphical methods for its determination, however, assume the existence of a logarithmic region, which may not occur near to a step change in roughness.

For the numerical solution of the discretized momentum equation at axial station x_P, the integration step size (x_P-x_A) determines the rate at which the longitudinal coordinate x is swept along the duct. In the vicinity of the boundary layer

leading edge ($x \approx 0$), the dependent variable f ($f=u,k,e,$) varies more rapidly with x, if one considers the initial growth rate of the boundary layer. Therefore, the use of a small but constant value for (x_P-x_A) could be appropriate for the rapid changes of f in the developing region but would imply in an excessive number of integration steps at the subsequent developed region. Likewise, a large value for (x_P-x_A) in the beginning of the sweep could, at the inlet region, cause numerical instability due to the large variation of all dependent variables within initial boundary layer development.

In this work, the integration step size was adopted as proportional to the distance from the point in question to the beginning of the calculation as:

$$\frac{x_P - x_A}{H} = \left[\frac{x - x_I}{x_L - x_I}\right]^b \tag{19}$$

where indexes "I" and "L" correspond to the initial and final x positions, respectively, H is one half of channel height and b is a constant.

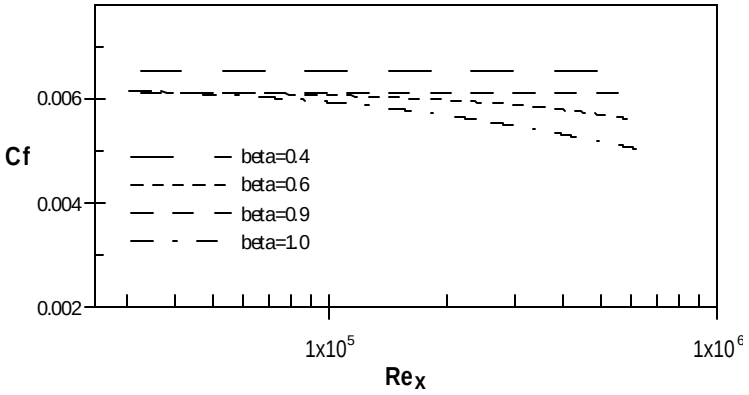

Figure 10 – Predictions of skin friction coefficient for different values of b in (19).

Further, in Eq. (19) the parameter b gives great flexibility for changing the integration step size. For $b=1$, a linear variation along the longitudinal coordinate is obtained. For $b>1$, the integration step varies more slowly in the inlet region. The effect of β on the numerical solutions is shown in Figure 9. Once can see that by reducing the value of β in equation (19) larger step sizes are computed in the beginning of the boundary layer development, leading to substantial variation on the value of C_f further downstream.

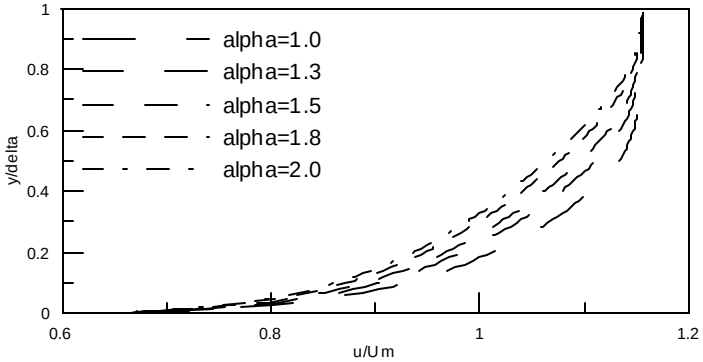

Figure 11 –. Velocity profiles for different values of a in Eqn. (20), station x=1.2m.

Regarding the transversal distribution of nodal points, at the boundary layer close to the wall, the discretization of the production term for k, equation (6), is rather sensitive to the transverse grid layout. A flexible grid point distribution is obtained by the use of a coordinate transformation of the type $f=(y')^{\alpha}$, giving for discrete positions along the transversal coordinate,

$$y'_i = \left(\frac{(H/2)^a}{N} + (y'_{i-1})^a \right)^{1/a} \tag{20}$$

where "*i*" in (20) is the index of the nodal point, a a parameter for grid control and $y'=H/2-y$ is the distance from the symmetry line, located halfway to the top surface ($H/2$), to the point in question. Therefore, nodal point "i" is located at distant y'_i from the domain centerline.

Thus, Figure 11 indicates that by changing the location of the grid points along the transverse wall coordinate, by means of varying α in equation (20), considerably different velocity profiles are obtained at the same x-station. Figures 10 and 11 ultimately indicate that care must be exercised when using a numerical procedure for calculating fluid flow. Final predictions must always be grid independent and optimal number and location of grid points should be sought as a way of reducing numerical uncertainties.

4. Concluding Remarks

This work presented computations with the standard *equation* k-ε model for simulation of turbulent boundary layer flows that present abrupt changes in the surface roughness.

Comparisons with experimental data indicated a reasonable agreement. More specifically, for surfaces subjected to sudden changes in roughness, demonstrated that the methodology here employed gave better or comparable results than those calculated with more sophisticated numerical tools and employing more elaborated turbulence modes. Accuracy of the calculated skin friction coefficient is also limited in the region where the displacement in origin is still adjusting itself to the new surface.

Essentially, the work herein suggests that, for accurate prediction of simple flows, proper implementation of the numerical model and the robustness and stability of the algorithm employed are important factors to be considered. Accordingly, for boundary layer flows, isotropic turbulence theories and simple parabolic codes can provide an economical and reliable tool during preliminary steps in the overall design process of engineering equipment, moreover, when using marching-forward techniques for flow simulations over surfaces with abrupt changes in roughness, it is noticed that the algebraic expressions that describe the growth of the displacement in origin lead to more accurate predictions.

5. Acknowledgement

The authors are thankful to NSF of USA and CNPq, Brazil, for their financial support during the preparation of this work.

6. References

Antonia, R.A. and R.E.Luxton, 1971. The Response of a Turbulent Boundary Layer to a Step Change in Surface Roughness Part 1. Smooth to Rough, *J. Fluid Mechanics*, Vol. 48, pp. 721-761.

Antonia, R.A. and R.E. Luxton, 1972. The Response of a Turbulent Boundary Layer to a Step Change in Surface Roughness Part 2. Rough to Smooth, *J. Fluid Mechanics*, Vol. 53, pp. 734-757.

Avelino, M.R., 1996, Sobre a Modelagem Diferencial de Camadas Limite Turbulentas com Transpiração, Msc. Thesis, PEM/COPPE/UFRJ.

Avelino, M.R., 2000. *Caracterização da Camada Limte Turbulenta Sujeita a Variações Abruptas de Propriedades na Superfície*, D.Sc. Thesis, PEM/COPPE/UFRJ. Rio de Janeiro.

Avelino, M.R., Silva Freire, A.P. and Kakac S., 2001. Experimental Determination of Velocity and Temperature Roughness Functions in Turbulent Boundary Layer Flows, *International Conference on Computational Heat and Mass Transfer*, Anais on CD.

Avelino, M.R., deLemos M.J.S. and Kakac S., 2001. Numerical Simulation of Turbulent Flow over Surfaces Subjected to Sudden Changes in Roughness, XVI Congresso Brasileiro de Engenharia Mecânica (COBEM).

Avelino M.R. and deLemos M.J.S., 2001. Numerical Study of Turbulent Flow Subjected to Sudden Changes in Wall Roughness, IV Meeting on Computational Modelling, Proc. of IVEMC, Vol.1, pp. 189-198, Nova Friburgo, RJ.

Avelino, M.R., Menut, P.P.M., Silva Freire, A.P., 1998. Experimental Characterization of a Turbulent Boundary Layer Subjected to a Step Change in Surface Roughness, *Proc. of 3rd Braz. Therm. Sci. Meet.* , Vol. II, pp. 1369-1374, Rio de Janeiro, RJ, Brazil.

Avelino, M.R., Menut, P.P.M., Silva Freire, A.P., 1999, Characteristics of the Turbulent Boundary Layer Over Surfaces with Abrupt Variation in Properties, *Trends Heat Mass Transf.*, Vol. 5, pp. 63-80.

Avelino, M.R., Kakac, S., and de Lemos, M.J.S., 2001, Numerical Study Of Turbulent Flow Subjected To Sudden Changes In Wall Roughness *Proc. of COBEM02 - 14th. Braz. Congr. Mech. Eng*, Uberlandia, Brazil, Nov. 22-26.

Avelino, M.R. and Marcelo J.S. de Lemos, 2001. Numerical Study of Turbulent Flow Subjected to Sudden Changes in Wall Roughness, *IV Meeting on Computational Modelling, Proc. of IVEMC*, Vol.1, pp. 189-198, Nova Friburgo.

Bandyopadhyay, P.R., 1987, "Rough Wall Turbulent Boundary Layers in the Transition Regime", J. Fluid Mechanics, Vol. 180, pp. 231-266.

Braga, E.J., de Lemos, M.J.S., 1999, Numerical Analysis of Coaxial Turbulent Jets in Diffusers and Contractions, *Proc. of COBEM99 - 13th. Braz. Congr. Mech. Eng.*, Águas de Lindóia, SP, Brazil, Nov. 22-26.

Coleman, H.W., R.J. Moffat and W.M. Kays, 1976, "Momentum and Energy Transport in the Accelerated Fully Rough Turbulent Boundary Layer", Report No. HMT-24, Stanford University.

de Lemos, M.J.S., Milan, A., 1997, Mixing of Confined Coaxial Turbulent Jets in Ducts of Varying Cross Section, *Proc. of COBEM97 - 12th. Braz. Cong. Mech Eng.*, Bauru, São Paulo, Brazil, December 8-12.

Guimaraes, J.H.D., S.J.F. Santos Jr., J. Su and A.P. Silva Freire, 1999, "The Turbulent Boundary Layer Subjected to a Sudden Change in Surface Roughness and Temperature", Proc. IMECE99, Tennesse, USA.

Jones, W.P., Launder, B.E., 1972, The Prediction of Laminarization with a Two-Equation Model of Turbulence, *Int. J. Heat & Mass Transfer*, vol. 15, pp. 301-314.

Kaplun, S., 1967, Fluid Mechanics and Singular Perturbations, Academic Press.

Launder, B.E., Spalding, D.B., 1972, Lectures in Mathematical Models of Turbulence, Academic Press, New York.

Launder, B.E., Spalding, D.B., 1974, The Numerical Computation of Turbulent Flows, *Comp. Math. App. Mech. Eng.*, vol. 3, pp. 269-289.

Ligrani, P.M., R.J. Moffat and W.M. Kays, 1979, "The Thermal and Hydrodynamic Behaviour of Thick Rough-Wall Turbulent Boundary Layers", Report No. HMT-29, Vol. 105, pp. 146-153.

Ligrani, P.M., R.J. Moffat and W.M. Kays, 1983, "Artificially Thickened Turbulent Boundary Layers for Studing Heat and Skin-Friction on Rough Surfaces", J. Fluids Engineering, Stanford University.

Ligrani, P.M., and R.J. Moffat, 1985, "Thermal Boundary Layers on Rough Surface Downstream o Steps in Wall Temperature", Int. J. Heat Mass Transf., Vol. 31, pp. 127-147.

Matsumoto, E., de Lemos, M.J.S., 1990, Development of an Axi-Symmetric Mixing Layer in A Duct of Constant Cross Section, *Proc. of 3rd Braz. Therm. Sci. Meet.*, vol. I, pp. 381-385, Itapema, Brazil, December 10-12.

Moore, W.L., 1951. "An Experimental Investigation of the Boundary Layer Developing Along a Rough Surface", Ph.D Thesis, State University of Iowa.

Nikuradse, J., 1933, "Stromungsgesetze in Rauhen Rohren", V.D.I. Forshungsheft, No. 361.

Patankar, S.V., 1980, Numerical Heat Transfer and Fluid Flow, McGraw Hill.

Patankar, S.V., 1988, Parabolic Systems, Chapter 2 of Handbook of Numerical Heat Transfer, Rohsenow *et al* Ed., John Wiley & Sons, NY.

Patankar, S.V., Spalding, D.B., 1972, A Calculation Procedure for Heat, Mass and Momentum Transfer in Three-Dimensional Parabolic Flows, *Int. J. Heat & Mass Transf.*, vol. 15, pp. 1787-1806.

Perry, A.E. e Joubert, P.N., 1963. Rough-Wall Boundary Layers in Adverse Pressure Gradients, J. Fluid Mech., Vol. 17, pp. 193--211.

Perry, A.E., K.L. Lim and S.M. Henbest, 1987. J. Fluid Mech., Vol. 177, pp. 437-466.

Silva Freire, A.P., Hirata, M.H., 1990. Analysis of Thermal Turbulent Boundary Layers over Rough Surfaces, Proc. *Proc. of 3rd Braz. Therm. Sci. Meet.*, vol. I, pp. 381-385, Itapema, Brazil

Thompson, R.S., 1978, "Note on the Aerodynamic Roughness Length for Complex Terrain", J. Applied Meteorol., Vol 17 pp. 1402-1403.

Wood, D.H. and Antonia, R.A., 1975, Measurements in a Turbulent Boundary Layer over a d-Type Surface Roughness, *J. Applied Mechanics*, Vol 53 pp. 591-596.

7. Nomenclature

A_{calc}	calculated duct area
A_{duct}	physical duct area
c_f	ϕ=1,2,μ_t model constants
E	Wall Law constant
k	Turbulent kinetic energy per unit mass, $\overline{u_i u_i} / 2$
N	Number of grid points in transverse direction
P	Production rate of k, Eq. (**6**)
p	Static pressure
H	Height of computational domain
Re	Reynolds number
S_ϕ	Source term for ϕ, ϕ=u,k,ε
u	Axial velocity
U^*	Friction velocity
U_m	Mean velocity
v	Transverse velocity
x	Axial coordinate
y	Wall distance,

Greek Letters

ε	Dissipation rate of k
μ_t	Turbulent momentum transport coefficient, Eq.(**4**)
ρ	Fluid density
μ_{eff}	Effective transport coefficient for u, Eq.(**3**)
μ	Fluid dynamic viscosity
Γ^ϕ_{eff}	Effective transport coefficient for ϕ, ϕ=u,k,ε
σ_k	Turbulent Prandtl/Schmidt number for k
σ_ε	Turbulent Prandtl/Schmidt number for ε
Ψ	Stream function
Ψ_I	Value of Ψ at internal surface of boundary layer
Ψ_E	Value of Ψ at external surface of boundary layer
K	Von Kármán constant
ϕ	General dependent variable, ϕ=u,k,ε
Ψ_{EI}	Ψ_E - Ψ_I
τ_w	Wall shear stress